Journal of Data Acquisition and Processing
ISSN: 1004-9037
https://sjcjycl.cn/
DOI: 10.5281/zenodo.777435

KALMAN BUCY REGION ADJACENT AND BIVARIATE CORRELATED CLASSIFICATION FOR DISASTER MANAGEMENT WITH SATELLITE IMAGES

M.Nirmala*
Assistant Professor, Hindusthan College of Engine*ering & Technology, Coimbatore*
nilarangan@gmail.com

V.Saravanan
Professor and Head, Department of Information Technology, Hindusthan College of Arts and Science , Coimbatore, vsreesaran@gmail.com

ABSTRACT

Over the recent few years, satellite systems and image analysis mechanisms have evolved to a scope where commercial Earth-observation instruments come up with notably to aid the management of crucial natural and technical disasters. Upon comparison with today's accessibility of satellite imagery to the circumstances about ten years ago, the quantity, promptness and obtain-ability of satellite imagery covering a definite calamity state of affairs has boosted in a significant manner. In this work, a novel Kalman Bucy Region Adjacent and Bivariate Correlated Classification (KBRA-BCC) method is proposed for image classification to perform an efficient disaster management event. The Kalman Bucy Region Adjacent and Bivariate Correlated Classification (KBRA-BCC) method is split into three sections. They are, image denoising, image segmentation and image classification for disastrous area identification. With the input image obtained from satellite image database, first, a Kalman–Bucy Image Denoising process is carried out to eliminate noisy pixels therefore improving the PSNR. With the processed image, second, Region Segmentation process is performed by employing Region Adjacency Gray Level Image Segmentation that splits the processed image into different segments with respect to two distinct features, color and intensity. Finally, with the segmented images, Bivariate Correlated Classification is employed to perform correlation between input and training image (i.e., disastrous image) that in turn classifies the segmented image into disastrous image or non-disastrous image. By employing Bivariate Correlated Classification assists in performing efficient disaster management with better accuracy and minimal time consumption. The subjective and objective evaluation, as well as the peak signal to noise ratio (PSNR) along with the segmentation time and classification accuracy, is compared, respectively, showing that the KBRA-BCC method can effectively enhance the disaster management with satellite images.

* ***M.NIRMALA,*** *Department of Computer Applications, Hindusthan College of Engineering & Technology, Anna University, Coimbatore, India, Mobile No 9952881646. E-mail : nilarangan@gmail.com*

Keywords: Disaster Management, Kalman–Bucy, Image Denoising, Region Adjacency, Gray Level, Image Segmentation, Bivariate Correlated Classification

1. Introduction

Over the past few years, satellite systems and image-analysis methods have developed to a magnitude where civil and commercial Earth-observation appliances can bestow efficiently to underpin the management of crucial technical and natural disasters, together with humanitarian calamity circumstances. On contrast to today's accessibility of satellite imagery to the state of affairs about ten years ago, the frequently, promptness and obtainability of satellite imagery sheathing an explicit catastrophe condition has enhanced considerably. There are numerous reasons that have led to this fact.

A new framework was introduced in [1] for reducing both the quantification and uncertainty involved in participatory damage assessment. The entire damage state classification process was split into straightforward micro-tasks by means of questionnaire survey with the objective of reducing both the complexity and subjectivity. Moreover, an information-theoretic model was also introduced depending on the maximum posteriori probability estimation for accurate probabilistic description. However, image denoising was not carried out in efficient manner.

A Satellite Precipitation-based Extreme Event Detection (SPEED) method was introduced in [2] to support the parametric or index insurance instruments for minimizing the flood risk. Here, the financial tools were also employed to assist in fast payouts in aftermath of disastrous event. SPEED model also measured hazard parameters however the computational complexity was not reduced by SPEED model.

A new multi-hazard disaster methodology was introduced in [3] to combine the experiment–simulation–field data. The methodology aimed on three dimensions with multi-hazard coupling, and emergency management. The designed methodology included experiments, multi-hazard field investigation, scenario analysis and response. But, here image pre-processing was not performed in a significant manner via multi-hazard disaster methodology. An integrated methodology was introduced in [4] for mapping flood extent and depths depending on Synthetic Aperture Radar (SAR) images and digital elevation model (DEM). But, segmentation was not carried out in efficient manner by integrated methodology.

2. Objective and Contributions

Our study aims to accurately and precisely delineate disastrous and non-disastrous images from satellite imagery. We develop an end-to-end Kalman–Bucy Image Denoising model based on unmeasured states and the actual process outputs. With this processed resultant output images, Region Adjacency Gray Level Image Segmentation is performed to split the processed images according to two different characteristics color or intensity. Finally, classification of disastrous and non-disastrous images is made by utilizing Bivariate Canonical Correlation classification model. Following the research line of previous works Majority-Vote based model for citizen-driven post-

disaster damage assessment [1] and Satellite Precipitation-based Extreme Event Detection (SPEED) [2], several modifications are introduced to such a method to further enhance its performance and applicability for robust disaster management. The key contributions of our paper are the following:

- Kalman–Bucy Disaster Image Filtering-based preprocessing is studied where the processed images are obtained in a computationally efficient manner by means of Kalman–Bucy function.

- To develop an algorithm called Region Adjacency Gray Level Image Segmentation using average intensity and root mean square deviation of pixel set for acquiring robust segmented images, therefore minimizing the segmentation time.

- To implement an algorithm called Bivariate Canonical Correlated classification using cross covariance matrix of segmented images to manage the disaster in a precise manner, hence classifying the output images into disastrous or non-disastrous image.

Extensive simulation results demonstrate that the proposed Kalman Bucy Region Adjacent and Bivariate Correlated Classification (KBRA-BCC) achieves better disaster management in terms of execution time, classification accuracy and false positive rate in comparison with the other disaster management methods.

2. Literature Survey / Related Work

Abrupt changes in climate and population growth in urban areas are creating risk of both persons and infrastructure leading to disasters. However, there still remains a gap in comprehending the extension of hidden geospatial biases that in turn influences the risk. Therefore there necessitates methods and materials to circumvent the issues arising due to disaster. Potential concerns from data science and social perspective was discussed in [5]. In [6], disaster events concerning intensity were designed by means of numerical simulation. Moreover, an automatic method for damaged building detection was also designed.

Over the past three decades, a great level of evolution in terms of volume, quality and quantity of satellite observations has occurred. A review of prevailing Earth Observing (EO) systems frequently utilized for estimating earthquake and crustal deformation and their potential hazard were investigated in [7]. On the basis of the review of literature and examples of studies conducted in the domain of coastal, hydro-meteorological and geohazards, a review of space-based Earth observations were potentially discussed in [8] with their requirements for disaster risk management. However, early evaluation and drought detection can ensure guidance for efficient water resources management.

In [9] multilayer perceptron neural network (MLPNN) was employed for efficient forecasting of drought. Also a detailed investigation using time series data

collected from Northern Area and KPK (Pakistan) was also made. However, landslide even collection in inventories are still said to be laborious and cumbersome process globally owing to the inconsistency or absence of landslide reporting. A detailed report was provided in [10] for landslides.

Since 2000s, the frequency and scalability of natural hazards are said to be in the increasing trend generating immense losses and deaths globally. Several natural hazards not only create huge issues to the disaster prevention and mitigation potentiality of infrastructure but also generate severe demands for rescue and recovery response. However, still there remain numerous disaster management obstacles.

Automated landslide detection using machine learning techniques was proposed in [11]. Deep learning-based materials and methods can bestow state of the art accuracy for remote sensing, therefore improving remote sensing potentialities for disaster management applications. To this end, the article in [12] concentrated on the significant classification of aerial image for emergency monitoring applications. With this accuracy was said to be improved. In [13], disaster prevention and alleviation for infrastructure, their advancements, ultimatum involved and opportunities were discussed. Certain remote sensing techniques for disaster management involving coastal areas were designed in detailed in [14].

In a catastrophe circumstances, the prevailing materials and methods designed on the basis of the change detection for road damage are said to be laborious and cumbersome to attain owing to the discrepancy of several data sources, specifically involving rural areas where pre-disaster remote sensing imagery are impenetrable to acquire. In [15], novel method on the basis of the Tracking, Learning, and Detector (TLD) framework for damaged road region detection from high-resolution remote sensing image was proposed that in turn ensured greater amount of feasibility. Certain requirements for applying satellite remote sensing towards disaster management by utilizing holistic factors based on case studies in central Asia was investigated in [16].

The usage of social media for information sharing has gained wide popularity. With these evolutions, the extent of data acquired increases daily in distinct types, namely, text, audio, video, and images. Despite these popularities, activities concerning Disaster Response (DR) are specifically depended on information obtained in a textual fashion, like, reports and email content, and hence the advantage of other media is frequently not gained. Deep Learning (DL) techniques also in the recent years and their application to DR have gained much advantage.

A systematic review of different numbers of articles concerning, current and future challenges, and their advantages utilizing DL for DR tasks was reviewed in [17]. Recent achievement and novel challenges for meteorological disaster management was reviewed in detail in [18]. Yet another extensive review of different

methods for evaluating disaster detection methods was investigated in [19]. The impact of the model frameworks on the landslide detection results were analyzed, and also the accuracy of deep belief networks (DBN) and convolutional neural network (CDN) models in addressing landslide problems were also compared. Here, the detection accuracy was improved with minimum error.

Motivated by the above materials and methods in this work, a Kalman Bucy Region Adjacent and Bivariate Correlated Classification (KBRA-BCC) method is proposed for disaster management.

3. Research Methodology

With the swift evolution of Earth observation techniques disaster management conducted by disaster managers now possess potential tools and techniques for collecting and integrating data in a cost efficient fashion. In this work a novel method called, Kalman Bucy Region Adjacent and Bivariate Correlated Classification (KBRA-BCC) is proposed for image classification to perform an efficient disaster management event. Figure 1 shows the block diagram of KBRA-BCC method.

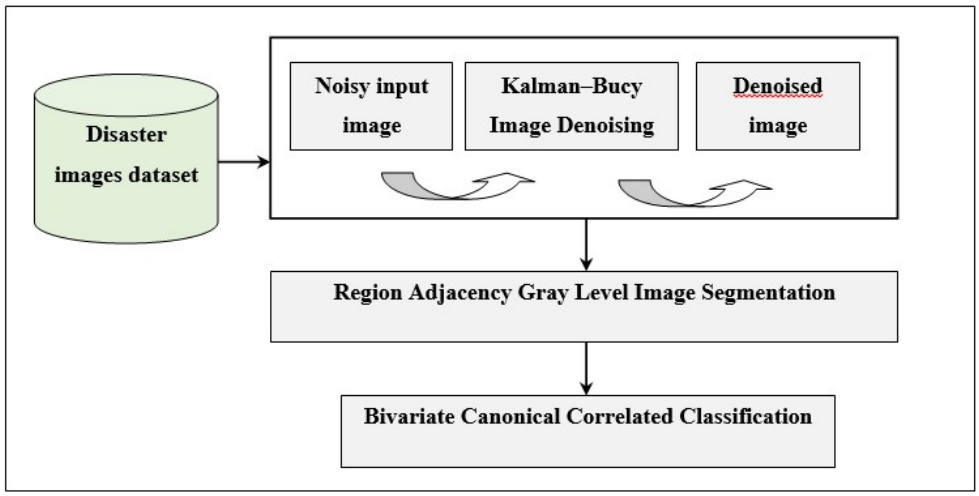

Figure 1 Block diagram of Kalman Bucy Region Adjacent and Bivariate Correlated Classification

As shown in the above figure, the KBRA-BCC method includes three processes, namely image denoising, image segmentation and image classification for disastrous area identification and management of the same. With the input images obtained from disaster image dataset, first image denoising is performed by means of Kalman–Bucy Image Denoising model. Second Region Segmentation process is performed based on two distinct features, color and intensity. Finally, Bivariate Correlated Classification model is utilized to perform correlation between input image and training image (i.e., disastrous image) with the objective of classifying segmented image into disastrous

image or non-disastrous image. With this efficient classification process is said to be achieved with better accuracy and minimal time consumption.

3.1 Kalman–Bucy Image Denoising model

Change in climatic conditions and exponential growth in population causes enormous issues to the habitation and well-being of planet Earth. The protection of its valuable environment and the retaliation to disasters when they happen both naturally and artificially is now exorbitant precedence. Technological innovations are amongst the most efficient solutions, and the speed and ease of satellite disaster monitoring has had a considerable influence on the efficiency of disaster response. Also, the utilization of satellite disaster early warning not only enhances the minimization of risk but also plans in case of restoration efforts in the wake of emergency.

The accuracy and efficiency of machine learning algorithms depend on the dataset being used for simulation and its clarity. Also not all the dataset are free from noise. Hence, a preliminary preprocessing has to be performed to eliminate the presence of noise. In our work, Kalman–Bucy Image Denoising model is employed to eliminate the noise on a controlled trajectory for four different types of natural disaster images, i.e., cyclone, earthquake, flood and wildfire. Figure 2 shows the structure of Kalman–Bucy Image Denoising model.

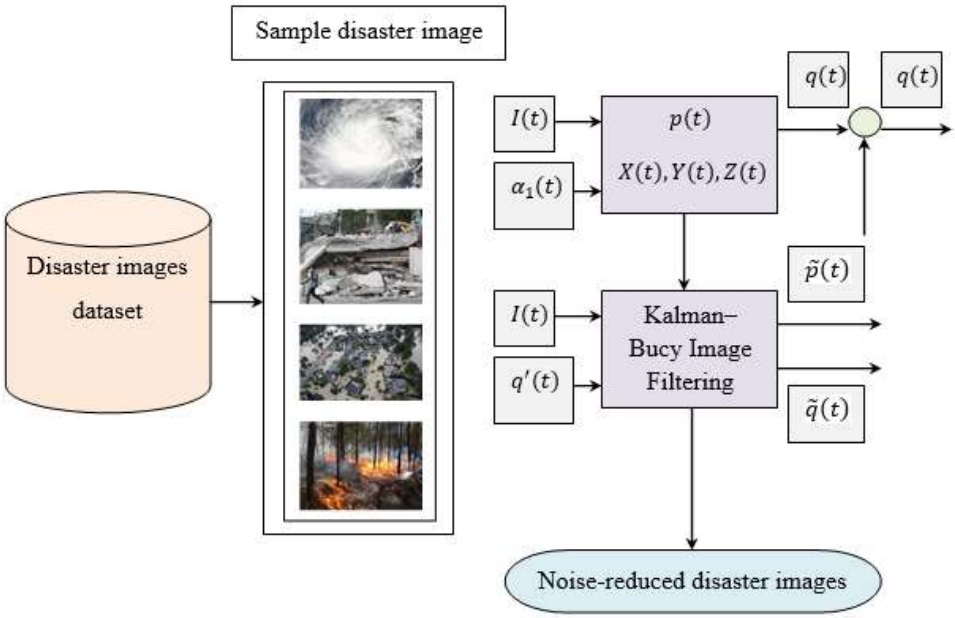

Figure 2 Structure of Kalman–Bucy Image Denoising model

As shown in the above figure, let us consider the linear continuous-time input disaster images 'I' from the disaster images dataset 'DS' subjected to controlled process. However, with the pixels on the controlled trajectory interrupted by noise, the ratio between maximum probable power of an image and the probable power of image are also said to be corrupted by noise. These noises are removed in our work

by means of Kalman–Bucy Image Denoising that is said to be written in the following state-space therefore enhancing the PSNR as given below.

$$p' = Xp + YI + \alpha_1 \quad (1)$$

$$q = Zp \quad (2)$$

$$q' = q + \alpha_2 \quad (3)$$

From the above equations (1), (2) and (3) 'I' represents the vector of disaster input images, 'p'' denotes the vector of actual states of the disaster input images, with 'q' specifying the vector of actual preprocessing and 'q'' representing the vector of measured processed outputs and 'α_1', 'α_2' denoting the process noise and output noise respectively. Then, given the disaster input images, measured processed outputs, assumed process and output noise, the objective of designing Kalman–Bucy Image Denoising remains in obtaining the unmeasured states and the actual process outputs (i.e., noise eliminated processed disaster images). This is illustrated in figure 1 where the estimated states are '$\tilde{p}(t)$', and estimated measured outputs are '$\tilde{q}(t)$' respectively. Then, the Kalman–Bucy Disaster Image Filtering estimate at time instance 't' is 'dq_t'' and the mean square filtering error '$Err(t)$' is mathematically formulated as given below.

$$PI = dq_t' = a(t)q_t'dt + \frac{Err(t)A(t)}{B^2(t)}[dp_t' - A(t)q_t'dt] \quad (4)$$

$$Err(t) = 2a(t)Err(t) + b^2(t) - \frac{Err^2(t)+A^2(t)}{B^2(t)} \quad (5)$$

From the above equations (4) and (5), Kalman–Bucy Disaster Image Filtering estimate results are obtained from 'dq_t'' based on the deterministic functions '$a(t)$', '$b(t)$', '$A(t)$', '$B(t)$' for the corresponding vector of measured processed outputs 'q_t'' and vector of actual states of the disaster input images 'dp_t'' respectively. Followed by which the Kalman–Bucy Disaster Image Filtering error '$Err(t)$' is obtained by differentiating with respect to deterministic functions respectively. In this manner noise reduced processed Disaster Images are obtained. The pseudo code representation of Kalman–Bucy Disaster Image Filtering-based preprocessing is given below.

Input: Disaster Images Dataset 'DS', Image '$I = I_1, I_2, .., I_n$'
Output: Noise-reduced Processed disaster images
1: **Initialize** time 't', process noise and output noise '$\alpha_1 = 0.01$', '$\alpha_2 = 0.02$' 2: **Begin** 3: **For** each Disaster Images Dataset 'DS' with Image 'I' 4: Obtain vector of actual states of the disaster input images as in equation (1) 5: Obtain vector of actual preprocessing as in equation (2) 6: Obtain the vector of measured processed outputs as in equation (3) 7: Evaluate Kalman–Bucy Disaster Image Filtering estimate as in equation (4) 8: Evaluate Kalman–Bucy Disaster Image Filtering estimate error as in equation (5) 9: **Return** processed disaster output Image 'PI' 10: **End for** 11: **End**

Algorithm 1 Kalman–Bucy Image Denoising-based Preprocessing

As given in the above algorithm with the objective of removing the noisy pixels from the input disaster images and also to improve the PSNR Kalman–Bucy Image Denoising model is used. In this algorithm with the disaster image dataset provided as input, actual states and measured processed outputs are obtained with which the Filtering estimate and Filtering estimate error are evaluated to produce noise-reduced processed disaster images. With the obtained noise-reduced processed disaster images segmentation are performed for further processing in the next section.

3.2 Region Adjacency Gray Level Image Segmentation

As given in the above section, with the processed images obtained as input, Region Adjacency Gray Level Image Segmentation is performed to split the pre-processed image (i.e., processed output) into distinct segments on the basis of the pixel in the specific region. Every pixel in a region is similar with respect to two different characteristics like color or intensity. In this work, a high-resolution Region Adjacency Gray Level Image Segmentation algorithm is proposed. Figure 3 shows the block diagram of Region Adjacency Gray Level Image Segmentation model.

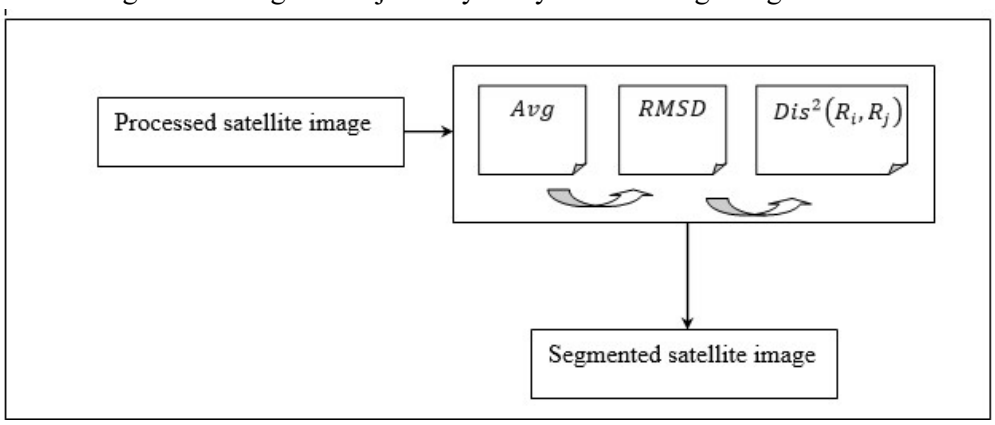

Figure 3 Block diagram of Region Adjacency Gray Level Image Segmentation model

As shown in the above block diagram, the Region Adjacency Gray associates distinct pixels via an edge, and each pixel region is scanned as a vertex. The edges between pixels are colored subject to their weights be in tune with their similarities between regions. The regions engulfed with dark edges are said to possess indistinguishable pixel features. On the other hand, the regions engulfed with light-colored edges possess distinct pixel features. Each region 'R_i' is distinguished by two criterions, i.e., 'Avg' the average intensity of set of pixel in the region and '$RMSD$' refers to the root mean square deviation of set of pixel in the region respectively. The average and root mean square deviation are mathematically stated as given below.

$$Avg = \frac{1}{n}\sum_{i=1}^{n} PI_i \tag{6}$$

$$RMSD = \sqrt{\frac{1}{n}\sum_{i=1}^{n}(PI_i - AVG)^2} \tag{7}$$

Next, at each circumference 'C_{ij}' refers to a set of adjoining regions '(R_i, R_j)' and an intensity distance '$Dis^2(R_i, R_j)$' as given below that is utilized in estimating the similarity between the intensity dispersal of two regions.

$$Dis^2(R_i, R_j) = \frac{(Bound_{R_i} + Boun\ \ _{R_j})(Avg_i, Avg_j)^2}{(Bound_{R_i} * RMSD_i^2) + (Bound_{R_j} * RMSD_j^2)} \quad (8)$$

From the above equation (8), '$Bound_{R_i}$' and '$Bound_{R_j}$' represents the boundary pixels that were eliminated forming gray scale pixels. With the obtained gray scale pixels, the average intensity is evaluated for regions with homogeneous gray levels, therefore differentiating between dark edges and light-colored edges. This is mathematically stated as given below.

$$SI = \begin{cases} if\ Avg < Dis^2(R_i, R_j), \text{dark edges} \\ if\ Avg > Dis^2(R_i, R_j), light - colored\ edges \end{cases} \quad (9)$$

With the resultant above segmented images 'SI' based on region factors, efficient differentiation between dark edges and light-colored edges are made, therefore minimizing the segmentation time. The pseudo code representation of Region Adjacency Gray Level Image Segmentation is given below.

Input: Disaster Images Dataset 'DS', processed disaster output Image 'PI'
Output: Computationally efficient segmented images
1: **Initialize** time 't' 2: **Begin** 3: **For** each processed disaster output Image 'PI' 4: Evaluate average intensity of set of pixel in the region as in equation (6) 5: Evaluate root mean square deviation of set of pixel in the region as in equation (7) 6: **For** each set of adjoining regions '(R_i, R_j) 7: Estimate intensity distance as in equation (8) 8: **End for** 9: **If** '$Avg < Dis^2(R_i, R_j)$' 10: **Then** the images form dark edges 11: **End if** 12: **If** '$Avg > Dis^2(R_i, R_j)$' 13: **Then** the images form light-colored edges 14: **End if** 15: **Return** segmented images 'SI' 16: **End for** 17: **End**

Algorithm 2 Region Adjacency Gray Level Image Segmentation algorithm

As given in the above Region Adjacency Gray Level Image Segmentation algorithm with two distinct features like, color and intensity, Region Adjacency is first determined. Second, with the identified Region Adjacency for each processed disaster output Image 'PI' intensity distance is evaluated. Finally, comparison is made between the average intensity of set of pixel in the region and intensity dispersal of two regions with which the segmented images into dark edges and light-colored edges are obtained with minimum segmentation time.

3.3 Bivariate canonical Correlated classification model

Finally, with the segmented images as input, in this section, a Bivariate Canonical Correlation classification model is designed for ensuring accurate disaster management. The Bivariate Canonical Correlation classification model is employed in our work to perform correlation between input image and training image (i.e., disastrous or non-disastrous image) for classifying the segmented image into disastrous or non-disastrous image. Figure 4 shows the structure of Bivariate Canonical Correlated classification model.

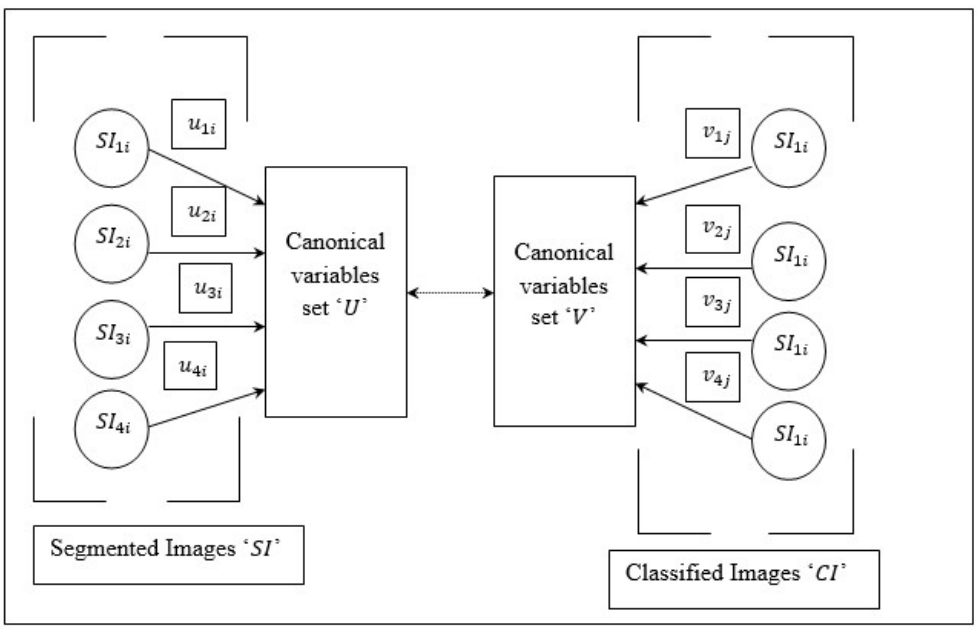

Figure 4 Bivariate Canonical Correlated classification model

As shown in the above figure, with four different types of disaster segmented images (i.e., cyclone, earthquake, flood and wildfire) as input (i.e., '$SI_{1i} = cyclone\ images$', '$SI_{2i} = earthquake\ images$' '$SI_{3i} = flood\ images$' and '$SI_{4i} = wildfire\ images$'), the objective remains in identifying a linear projection of set '$segmented\ image\ SI$' and '$classified\ image\ CI$' by maximizing linear correlation between two sets of new canonical variables 'U' and 'V'. Here, '$i = 1,2, \ldots n$' and '$j = 0\ or\ 1$'. Given

two column vectors '$SI = \{SI_1, SI_2, \dots, SI_n\}'$' and '$CI = \{CI_1, CI_2, \dots, CI_m\}'$' the Bivariate Canonical Correlated classification identifies vectors '$u \in R^n$' and '$v \in R^m$' such that the random variables '$u^T SI$' and '$v^T CI$' maximize the correlation as given below. First, the cross covariance matrix is mathematically stated as given below.

$$\Sigma_{SI,CI} = COV(SI, CI) \tag{10}$$

$$\rho = CORR(u^T SI, v^T CI) \tag{11}$$

Then, the random variables '$U = u \in R^n$' and '$V = v \in R^m$' represents the initial canonical variable pair (i.e., '$SI_{1i} = cyclone\ images$') and so on. When the correlation value ranges between '-1' and '0', the image is said to be non-disastrous image and on the other hand, if the correlation value ranges between '0' and '1', the image is said to be disastrous image. The pseudo code representation of Bivariate Canonical Correlated classification is given below.

Input: Disaster Images Dataset 'DS', processed disaster output Image 'PI'
Output: Accurate disaster management
1: **Initialize** column vectors '$SI = \{SI_1, SI_2, \dots, SI_n\}'$' and '$CI = \{CI_1, CI_2, \dots, CI_m\}'$' 2: **Initialize** variables 'U' and 'V' 3: **Begin** 4: **For** each segmented images 'SI' 5: Evaluate cross covariance matrix as in equation (10) 6: Evaluate Bivariate Canocial Correlated classification as in equation (11) 7: **If** '$\rho\ ranges\ between - 1\ and\ 0$' 8: **Then** the segmented image is non-disastrous image 9: **End if** 10: **If** '$\rho\ ranges\ between\ 0\ and\ 1$' 11: **Then** the segmented image is disastrous image 12: **End if** 13: **End for** 14: **End**

Algorithm 3 Bivariate Canonical Correlated classification

As given in the above Bivariate canonical Correlated classification algorithm, with the objective of improving the results of disaster management, analysis of canonical correlation is made between the segmented input images and the classified output images via cross covariance matrix. With the resultant cross covariance matrix values, Bivariate canonical Correlated classification is made to obtain the actual classified output. Finally, with the classified output, statistical evaluation is made to obtain the output as disastrous or non-disastrous image accurately.

3. Experimental setup

The proposed Kalman Bucy Region Adjacent and Bivariate Correlated Classification (KBRA-BCC) method is explored and tested with other significant methods, namely Majority-Vote based model for citizen-driven post-disaster damage assessment [1] and [Satellite Precipitation-based Extreme Event Detection (SPEED) [2]. A persuading characteristic for the assessment metric is their potentiality to differentiate between results of different building detection methods developed and simulation in MATLAB using the disaster images dataset, https://www.kaggle.com/mikolajbabula/disaster-images-dataset-cnn-model.

Experimental evaluation of Kalman Bucy Region Adjacent and Bivariate Correlated Classification (KBRA-BCC) method is carried out on the factors such as peak signal-to-noise ratio, segmentation time, and classification accuracy with respect to a number of satellite images. The efficiency of the disaster management method is determined by estimating the method numerous execution measures or by monitoring the performance by several performance metrics. For the proposed work the method is validated in terms of:

- Peak signal-to-noise ratio
- Segmentation time
- Classification accuracy

4 Results and Discussions

4.1 Performance analysis of segmentation time

Segmentation time refers to the time consumed in segmenting the processed images. This is mathematically stated as given below.

$$Seg_{time} = \sum_{i=1}^{n} I_i * Time\left[Dis^2\left(R_i, R_j\right) + \text{differentiating between [dark and light} - \text{colored edges}\right] \quad (12)$$

From the above equation (12), the segmentation time 'Seg_{time}', refers to the time consumed in differentiating between dark and light colored edges 'differentiating between [dark and light − colored edges', estimating similarity between intensity dispersal of two regions '$Dis^2\left(R_i, R_j\right)$' with respect to the images provided as input for simulation 'I_i'. It is measured in terms of milliseconds (ms). Table 1 given below lists the segmentation time for three different methods, KBRA-BCC, Majority-Vote based model for citizen-driven post-disaster damage assessment [1] and SPEED [2].

Table 1 Segmentation time measure of the proposed KBRA-BCC PS method and other state-of-the-art methods

Number of images	Segmentation time (ms)		
	KBRA-BCC	Majority-Vote based model for citizen-driven	SPEED

		post-disaster damage assessment	
50	27.5	30	40
100	35.25	45.55	53.25
150	48.15	65.35	78.15
200	55.35	80.15	95.35
250	58.25	95.35	105.25
300	64.55	100.25	135.45
350	68.35	125.55	155.35
400	75.25	140.35	175.45
450	80.55	155.25	190.25
500	105.35	175.85	203.55

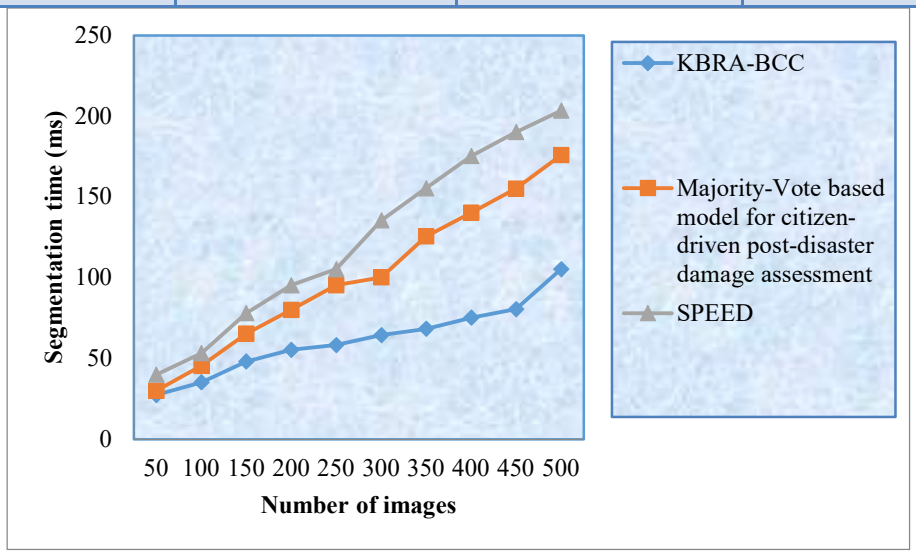

Figure 5 Segmentation time versus number of images

Figure 5 given above illustrates the graphical representation of segmentation time with respect to 500 distinct numbers of disaster images split into four categories, cyclone, earthquake, flood and wildfire obtained from the input dataset. In the above figure, the horizontal axis refers to the number of sample images involved in simulation and on the hand the vertical axis represents the segmentation time measured in terms of milliseconds (ms). From the above figure, the segmentation time is found to be directly increasing to the samples involved in the simulation process. In other words, with the increase in the number of samples images results in an increase in the number of light colored and dark colored edges and therefore increase in estimating the similarity between the intensity dispersal of two regions for managing disaster process. As a result, there is an increase in the segmentation time also. However, simulations performed with 50 samples showed segmentation time of 27.5 ms using KBRA-BCC method, 30 ms using [1] and 40 ms using [2] respectively. From these results, the segmentation time using KBRA-BCC method was found to be lesser comparatively than the state-of-the-art methods. The reason behind the improvement

was due to the application of Region Adjacency Gray Level Image Segmentation model. By applying this model, initially, two distinct features like, color and intensity were determined by means of Region Adjacency function. Next, with the determined Region Adjacency for each processed Image intensity distance were estimated. Finally, the actual comparison process was made between average intensity and intensity dispersal of two regions. With this the segmentation time involved using KBRA-BCC method were found to be comparatively lesser by 32% compared to [1] and 46% compared to [2].

4.2 Performance analysis of classification accuracy

Classification accuracy refers to the measure taken with which accurate classification is performed. In other words, classification accuracy refers to the accurate classification of disaster images made with which accurate disaster management is ensured. The accuracy is mathematically stated as given below.

$$CA = \sum_{i=1}^{n} \frac{I_{CA}}{I_i} \quad (13)$$

From the above equation (13), classification accuracy 'CA' is estimated on the basis of the disaster image involved in the actual simulation process 'I_i' and the images that are classified in an accurate fashion 'I_{CA}'. It is measured in terms of percentage (%).Table 2 given below list the classification accuracy for three different methods, KBRA-BCC, Majority-Vote based model for citizen-driven post-disaster damage assessment [1] and SPEED [2].

Table 2 Classification accuracy measure of the proposed KBRA-BCC PS method and other state-of-the-art methods

Number of images	Classification accuracy (%)		
	KBRA-BCC	Majority-Vote based model for citizen-driven post-disaster damage assessment	SPEED
50	92	90	88
100	90.35	88.15	85.35
150	87.45	86.25	83
200	85.25	83.25	80.25
250	83	80.45	75.35
300	81.45	78.25	72
350	78.35	75.15	70.15
400	76.45	73	68.25
450	75	70.45	65

500	73.15	68.25	63

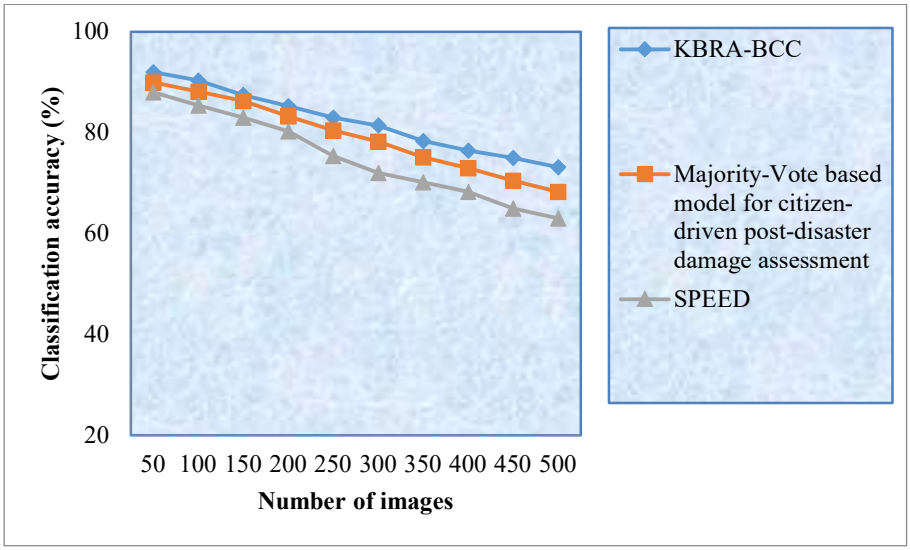

Figure 6 Classification accuracies versus number of image

Figure 6 given above shows the classification accuracy results obtained using the three methods, KBRA-BCC, Majority-Vote based model for citizen-driven post-disaster damage assessment [1] and SPEED [2]. From the above figure increasing the classification accuracy causes a significant amount of noise and this is in turn results in the decrease in the classification accuracy. However, simulations performed with 50 images found an improvement of 92% classification accuracy using KBRA-BCC, 90% classification accuracy using [1] and 88% of classification accuracy using [2] respectively. The improvement in the classification accuracy using KBRA-BCC was owing to the incorporation of Bivariate canonical Correlated classification algorithm. By applying this algorithm, first, canonical correlation analysis were made between segmented input and classified output images using cross covariance matrix. Next, with the results, Bivariate canonical Correlated classification was performed therefore obtaining the actual output. With this correlation, classification of images into disastrous or non-disastrous image were made in an accurate manner therefore improvement observed using KBRA-BCC by 4% compared to [1] and 10% compared to [2].

4.3 Performance analysis of false positive rate

Finally, the significant parameter required for disaster management is the false positive rate. This is because of the reason that certain images being normal are considered as disaster and vice versa. Hence, this misclassification has to be detected. False positive rate is mathematically stated as given below.

$$FPR = \sum_{i=1}^{n} \frac{I_{WD}}{I_i} * 100 \quad (14)$$

From the above equation (14), the false positive rate 'FPR' is measured based on the samples involved in the disaster management process 'I_i' and the samples wrongly detected as disaster though not to be 'I_{WD}'. It is measured in terms of percentage (%). Finally, table 3 given below provides the metric analysis of false positive rate analysis using KBRA-BCC, Majority-Vote based model for citizen-driven post-disaster damage assessment [1] and SPEED [2] respectively.

Table 3 False positive rate measure of the proposed KBRA-BCC PS method and other state-of-the-art methods

Number of images	False positive rate		
	KBRA-BCC	Majority-Vote based model for citizen-driven post-disaster damage assessment	SPEED
50	6	8	10
100	6.35	8.85	11.23
150	6.55	9.35	12.45
200	7	9.85	13.35
250	7.35	10.25	13.85
300	7.85	10.55	14.25
350	8.25	11	15
400	9.15	11.35	15.35
450	10.35	11.85	15.85
500	11	13	16

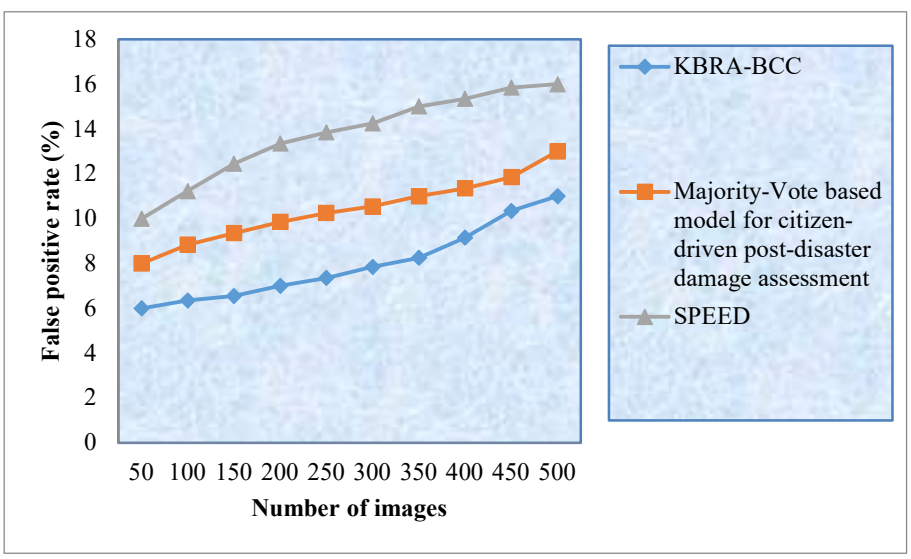

Figure 7 False positive rates versus number of image

Figure 7 given above shows the graphical representation of false positive rate with respect to differing samples. From the above figure, x axis represents the samples ranging between 50 and 500 and y axis represent the false positive rate. Also, increasing the images causes an increase in the false positive rate also. This is due to the reason that with the increase in the images, disaster present in satellite images for detection and management increases and this in turn also results in a significant amount of falsification of disaster management also. However, simulations conducted with 50 samples observed the false positive rate of 6% when applied with KBRA-BCC, 8% using [1] and 10% using [2] respectively. With this analysis, the false positive rate for KBRA-BCC method was found to be comparatively lesser than the state-of-the-art methods. The improvement was owing to the application of Kalman–Bucy Image Denoising-based Preprocessing algorithm. By applying this algorithm, the noisy pixels were removed or eliminated from the input disaster images via Kalman–Bucy function. Next, by utilizing actual states and measured processed outputs with which Filtering estimate and Filtering estimate error were obtained therefore producing noise-reduced processed disaster images that in turn reduced the false positive rate using KBRA-BCC method by 24% compared to [1] and 42% compared to [2] respectively.

5 Conclusion

In this paper, we proposed a novel Kalman Bucy Region Adjacent and Bivariate Correlated Classification (KBRA-BCC) method for building detection from satellite images. We developed the KBRA-BCC method by integrating Kalman Bucy Region Adjacent using similarity between the intensity dispersal of two regions and Bivariate Correlated Classification using canonical Correlated classification which first segments the processed satellite images and classifies image features more accurately. The reason behind the improvement was that first to remove the noise by preserving the geometrical features, preprocessing was performed by means of Kalman–Bucy Disaster Image Filtering-based model. Second with the processed images as input, Region Adjacency Gray Level Image Segmentation algorithm was applied that segmented the images into dark edges and light-colored edges in a significant manner using average intensity and root mean square deviation. Third, with the segmented images as input, Bivariate canonical Correlated classification algorithm was applied to differentiate between disastrous and non-disastrous images for disaster management. We used the Disaster Images Dataset for disaster management. The experimental result shows that the proposed disaster detection method achieved greater improvement in terms of both segmentation time and false positive rate with improved accuracy.

6 References

[1] Asim B. Khajwal and Arash Noshadravan, "An uncertainty-aware framework for reliable disaster damage assessment via crowdsourcing" International Journal of Disaster Risk Reduction, Elsevier, Volume 55, March 2021, Pages 1-15 [Majority-Vote based model for citizen-driven post-disaster damage assessment] https://doi.org/10.1016/j.ijdrr.2021.102110

[2] Annibale Vecere, Mario Martina, Ricardo Monteiro and Carmine Galasso, "Satellite precipitation–based extreme event detection for flood index insurance", International Journal of Disaster Risk Reduction, Volume 55, March 2021, Pages 1-15 [Satellite Precipitation-based Extreme Event Detection (SPEED)] https://doi.org/10.1016/j.ijdrr.2021.102108

[3] Rui Ba, Qing Deng, Yi Liu, Rui Yang and Hui Zhang, "Multi-hazard disaster scenario method and emergency management for urban resilience by integrating experiment–simulation–field data", Journal of Safety Science and Resilience, Volume 2, Issue 2, June 2021, Pages 77-89 https://doi.org/10.1016/j.jnlssr.2021.05.002

[4] Chen Hao, li P. Yunus, Srikrishnan Siva Subramanian and Ram Avtar, "Basin-wide flood depth and exposure mapping from SAR images and machine learning models", Journal of Environmental Management, Elsevier, Volume 297, 2021, Pages 1-15 https://doi.org/10.1016/j.jenvman.2021.113367

[5] Caroline M. Gevaert, Mary Carman, Benjamin Rosman, Yola Georgiadou, and Robert Soden, "Fairness and accountability of AI in disaster risk management: Opportunities and challenges", Volume 2, Issue 11, 12 November 2021, 100363, https://doi.org/10.1016/j.patter.2021.100363

[6] Luis Moya, Christian Geiß, Masakazu Hashimoto, Erick Mas , Shunichi Koshimura , and Günter Strunz, "Disaster Intensity-Based Selection of Training Samples for Remote Sensing Building Damage Classification", IEEE Transactions on Geo Science and Remote Sensing, Vol. 59, NO. 10, Oct 2021, DOI: 10.1109/TGRS.2020.3046004

[7] J. R. Elliott, "Earth Observation for the Assessment of Earthquake Hazard, Risk and Disaster Management", Surveys in Geophysics, Springer, Aug 2020, Volume 41, Issue 6, p.1323-1354 10.1007/s10712-020-09606-4

[8] G. Le Cozannet, M. Kervyn, S. Russo, C. Ifejika Speranza, P. Ferrier, M. Foumelis, T. Lopez, H. Modaressi, "Space-Based Earth Observations for Disaster Risk Management", Surveys in Geophysics, Springer, Mar 2020,Pages 1-27, https://doi.org/10.1007/s10712-020-09586-5

[9] Zulifqar Ali, Ijaz Hussain, Muhammad Faisal, Hafiza Mamona Nazir, Tajammal Hussain, Muhammad Yousaf Shad, Alaa Mohamd Shoukry, Showkat Hussain Gani, "Forecasting Drought Using Multilayer Perceptron Artificial Neural Network Model", Advances in Meteorology, Hindawi, Volume 2017, 9 pages May 2017, https://doi.org/10.1155/2017/5681308

[10] Caroline S. Juang, Thomas A. Stanley, Dalia B. Kirschbaum, "Using citizen science to expand the global map of landslides: Introducing the Cooperative Open Online Landslide Repository (COOLR)", PLOS ONE | https://doi.org/10.1371/journal.pone.0218657 July 3, 2019, https://doi.org/10.1371/journal.pone.0218657

[11] Sansar Raj Meena, Lucas Pedrosa Soares, Carlos H. Grohmann, Cees van Westen, Kushanav Bhuyan, Ramesh P. Singh, Mario Floris, Filippo Catani, "Landslide detection in the Himalayas using machine learning algorithms and U-Net", Landslides, Springer, Aug 2022, Pages 1-21, DOI 10.1007/s10346-022-01861-3

[12] Christos Kyrkou, and Theocharis Theocharides, "EmergencyNet: Efficient Aerial Image Classification for Drone-Based Emergency Monitoring Using Atrous Convolutional Feature Fusion", IEEE Journal of Selected Topics in Applied Earth Observations and Remote Sensing, Vol. 13, Aug 2020, Pages 1-14, DOI 10.1109/JSTARS.2020.2969809

[13] Dianyou Yu, Zheng He, "Digital twin-driven intelligence disaster prevention and mitigation for infrastructure: advances, challenges, and opportunities", Natural Hazards, Springer, Jan 2022, Pages 1-36, https://doi.org/10.1007/s11069-021-05190-x

[14] Yaw A. Twumasi, Edmund C. Merem, and Tomas Ayala-Silva, "Coupling GIS and remote sensing techniques for coastal zone disaster management: the case of Southern Mississippi", Geoenvironmental Disasters, Springer, Jul 2016, 10.1186/s40677-016-0056-7

[15] Kang Zhao, Jingjing Liu, Qingnan Wang, Xianjun Wu, Jihui Tu, "Road Damage Detection From Post-Disaster High-Resolution Remote Sensing Images Based on TLD Framework", IEEE Access, Apr 2022, Volume: 10, Page(s): 43552 – 43561, DOI: 10.1109/ACCESS.2022.3169031

[16] Kazuya Kaku, "Satellite remote sensing for disaster management support: A holistic and staged approach based on case studies in Sentinel Asia", International Journal of Disaster Risk Reduction, Elsevier, Feb 2019, Volume 33, Pages 417-432, https://doi.org/10.1016/j.ijdrr.2018.09.015

[17] Nilani Algiriyage, Raj Prasanna, Kristin Stock, Emma E. H. Doyle, David Johnston, "Multi-source Multimodal Data and Deep Learning for Disaster Response: A Systematic Review", Computer Science, Springer, Nov 2021, Pages 1-29, https://doi.org/10.1007/s42979-021-00971-4

[18] Peng Ye, "Remote Sensing Approaches for Meteorological Disaster Monitoring: Recent Achievements and New Challenges", International Journal of Environmental Research and Public Health, Mar 2022, doi: 10.3390/ijerph19063701

[19] Naina Said, Kashif Ahmad, Michael Riegler, Konstantin Pogorelov, Laiq Hassan, Nasir Ahmad, Nicola Conci, "Natural disasters detection in social media and

satellite imagery: a survey", Multimedia Tools and Applications, Springer, Jul 2019, Pages 1-36,https://doi.org/10.1007/s11042-019-07942-1

[20] Leijin Long, Feng He, Hongjiang Liu, "The use of remote sensing satellite using deep learning in emergency monitoring of high-level landslides disaster in Jinsha River", The Journal of Supercomputing, Springer, Feb 2021 , Pages 1-17, https://doi.org/10.1007/s11227-020-03604-4